Long Term Temporal Changes in Structure and Function of Rat Visual System After Blast Exposure

Daniel F. Shedd,[1] Nikolaus A. Benko,[1] Justin Jones,[2] Brian E. Zaugg,[3] Robert L. Peiffer, and Brittany Coats[1]

[1]Department of Mechanical Engineering, University of Utah, Salt Lake City, Utah, United States
[2]Department of Bioengineering, University of Utah, Salt Lake City, Utah, United States
[3]Department of Ophthalmology & Visual Sciences, University of Utah, John A Moran Center, Salt Lake City, Utah, United States

Correspondence: Brittany Coats, Department of Mechanical Engineering, University of Utah, 1495 E 100 S, 1550 MEK, Salt Lake City, UT 84112, USA; brittany.coats@utah.edu.

Submitted: January 20, 2017
Accepted: November 21, 2017

Citation: Shedd DF, Benko NA, Jones J, Zaugg BE, Peiffer RL, Coats B. Long term temporal changes in structure and function of rat visual system after blast exposure. *Invest Ophthalmol Vis Sci*. 2018;59:349–361. https://doi.org/10.1167/iovs.17-21530

Purpose. We identify long-term ocular sequelae subsequent to experimental blast exposure.

Methods. Male Long-Evans rats were exposed to 230 kPa side-on primary blast overpressure using a compressed air driven shock tube. Visual system function and structure were assessed for 8 weeks after exposure using optokinetic nystagmus and optical coherence tomography. Vitreous protein expression and histology (TUNEL, H&E) were performed at 1 day and 1, 4, and 8 weeks. IOP was recorded bilaterally during blast in a subset of animals.

Results. Blast pressure profiles resembled the Friedlander waveform indicative of an open field blast. Peak IOP in directly-exposed eyes (240 kPa) was similar to peak blast overpressure, but IOP in indirectly-exposed eyes was 30% lower. Contrast sensitivity of blast-exposed animals decreased significantly by 20% 1 day after blast and did not recover by 8 weeks. Significant swelling and structural damage to the corneal epithelial and stromal layers were observed 2 weeks after blast exposure. Swollen corneas increased 254 ± 143 μm from baseline by 6 weeks, and scarring developed by 8 weeks. Histology revealed additional lens pathology 1 week after blast, suggestive of cataract development. Endothelial cell density increased significantly in blast-exposed animals between 1 and 4 weeks. Neurofilament heavy chain significantly increased after blast and returned to near baseline values by 8 weeks. Inflammatory cytokine changes corroborated ocular pathology findings.

Conclusions. These data demonstrate immediate visual dysfunction and biochemical responses, but delayed structural pathology, in response to single primary blast exposure. The delayed pathology time course may provide a window to implement treatment strategies for improved visual outcome.

Keywords: ocular blast injury, cornea, retina, contrast sensitivity

Blast exposure is a leading cause of ocular injury in military personnel. Three recent military conflicts (Operation Enduring Freedom, Operation Iraqi Freedom, and Operation New Dawn) have resulted in visual system injury in 13% of all casualties.[1,2] Visual system impairment in soldiers subjected to blast exposure(s) often are caused by open globe injury, in which the outer shell of the eye has been torn, penetrated, or perforated. However, many soldiers have experienced closed globe injuries and visual system impairments that are not detected at health inspections immediately after the blast. In many cases, the visual impairment is related to traumatic brain injury (TBI). However, Mader et al.[3] reported 79 cases (nearly 40%) of soldiers with visual impairment who had no diagnosis of TBI. In cases without associated severe injuries, visual impairment may not be detected until months after the blast exposure. In these cases, blast pressure waves could create microstructural damage in the eye and initiate inflammatory pathways that lead to visual dysfunction months after blast exposure.

Animal models that capture the progression of ocular injury and visual dysfunction following blast exposure have been reported, but the methodology used in each of these models varies dramatically. For example, each study uses different animal species (mouse,[4] rat,[5] rabbit[6]), a different mechanism for blast generation (shock tubes,[7–9] paintball guns,[4] rifles,[10] and small magnitude explosives[9]), and focuses on different pressure magnitudes and durations. Rodents are a common choice because of their inexpensive cost, ability to perform visual behavior testing, and availability of genetic knockouts for exploring molecular mechanisms of injury. Hines-Beard et al.[4] exposed mice to one of three blast levels using a modified paintball gun.[4] The experimental setup created a long duration positive pressure wave (12–18 ms) with reflected blast overpressures of 163, 182, or 210 kPa. Visual acuity testing and optical coherence tomography (OCT) was performed at 3, 7, 14, and 28 days after blast. Visual ability decreased by 4 weeks after blast exposure, but was not statistically significant due to limited sample size. In general, it appeared that damage induced by the blast trauma still was progressing at the final time point 28 days after exposure. In 2013, Zou et al.[9] used open field explosion of five kg trinitrotoluene (TNT) to induce ocular trauma in rats. The explosive generated 480 kPa blast pressure at 2 m and 180 kPa at 3 m. Retinal thickness increased relative to control animals at 72 hours and 2 weeks after blast. Damage to the blood–retinal barrier was a suspected cause of

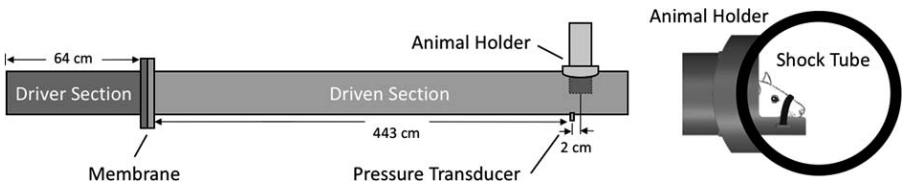

FIGURE 1. Schematic of holder and animal with relation to the shock tube. The right eye was exposed directly to a side-on blast. The sensor recording the tube pressure was located 2 cm upstream from the right eye.

the thickening due to increased VEGF, astrocytes, and glial fibrillary acidic protein (GFAP) in blood vessels.

More recently, Choi et al.[11] studied the effects of single and repeated blast overpressure on rats using immunohistochemistry analysis. A compressed air shock tube was used to deliver 70 kPa blasts (duration = 2 ms) to rats positioned inside the tube. Single blast-exposed rats were sacrificed 5 days after exposure. The repeated blast group underwent five blasts on consecutive days (one exposure per day) and were killed immediately after the final blast exposure. Repeated exposure led to increased caspase-3 expression and increased GFAP expression, with damage to the ganglion cell and inner nuclear layers of the retina.

These studies illustrate that ocular damage from blast can be recreated successfully in the laboratory with varying degrees of fidelity to the ideal Friedlander waveform.[12] Retinal thickening, retinal thinning, apoptosis, gliosis, optic nerve avulsion, and loss of photoreceptors are among injuries reported in these studies,[4,11] and injuries seen clinically in human patients.[13] Fewer studies have focused on the most anterior portion of the eye, such as the cornea. Hines-Beard et al.[4] noted corneal damage at 7 to 14 days after blast, but comprehensive tracking of the corneal response to blast is lacking. Furthermore, nearly all blast ocular studies to date have focused on injury sequelae less than 4 weeks after the blast. The exception to this is a study by Mohan et al.[14] evaluating chronic retinal ganglion cell function in different aged mice following blast exposure up to 10 months after blast. Based on the findings of Mohan et al.,[14] and those reported by Hines-Beard et al.,[4] visual system injuries appear to progress 4 weeks after blast. We evaluated rats for 8 weeks after blast exposure to double the length of time observed in the Hines-Beard study and capture a greater progression of injury.

The objective of this study was to identify ocular blast exposure sequelae up to 8 weeks. To achieve this objective, we experimentally reproduced open field primary blast ocular trauma in a rodent model, and quantified ocular structural changes, visual function, histology, and vitreal proteins. In addition, we measured in vivo IOP during blast exposure to quantify the difference between directly- and indirectly-exposed eyes. These longer-term studies elucidated the temporal progression of ocular impairment, and may help identify time-dependent diagnostic and treatment strategies for ocular trauma following blast exposure.

METHODS

Blast Exposure

All animal studies were reviewed by the Institutional Animal Care and Use Committee of the University of Utah and were performed in adherence to the ARVO Statement for the Use of Animals in Ophthalmic and Vision Research. Long-Evans rats (n = 54; 399 ± 68 g; age, 10–14 weeks) were administered carprofen orally (20 mg) 1 day before and 1 day after blast exposure for pain management. Inhaled isoflurane (5%) was administered for light sedation followed by intraperitoneal injection of ketamine (65 mg/kg) and dexmedetomidine (0.14 mg/kg). Anesthesia depth was assessed using toe pinch and eye touch reflexes. Rats were wrapped in a Kevlar shroud up to the neck and placed in a three-dimensional (3D) printed holder such that the right eye was exposed directly and the left eye was exposed indirectly to the blast (Fig. 1). The head was restrained using a Velcro strap to prevent excessive head motion. The animal was monitored from an external rear viewing port before and during the blast. Control animals (n = 38, 380 ± 53 g) were anesthetized similar to the blast-exposed animals but were not exposed to a blast.

A 230 kPa blast exposure with approximately a 7 ms positive phase duration was generated using a 521 cm long shock tube. This blast pressure is similar to the pressure used previously in rodent models by Hines-Beard et al.[4] and did not cause high mortality rates. A comparison of the blast parameters found in several types of improvised explosive devices was generated from explosive magnitudes from the National Ground Intelligence Center[15] and equations from Alonso et al.,[16] and is shown in Figure 2. According to those sources, the pressure and duration used in this study were estimated to be similar to a compact car bomb at a stand-off distance of 15 to 20 m. The tube had a 64 cm long driver section, 457 cm driven section, and constant internal diameter of 15 cm. The driver section was pressurized with compressed air until a 0.01-inch biaxially-oriented polyethylene terephthalate (BoPET) membrane ruptured. The animal was placed within the shock tube 455 cm from the driver section. At this location, the pressure profile had developed fully into a Friedlander waveform. Pressure located 2 cm upstream of the right eye was recorded for each blast-exposed animal at 1 Ms/s using a flush-mounted pressure sensor (PCB Piezotronics, Inc., Depew, NY, USA). The pressure time history profiles were filtered using a custom hardware anti-aliasing filter with f_c = 180 kHz, and recorded using NI DAQ 9223 into Labview (National Instruments, Austin, TX, USA). Blast pressures were also filtered post hoc using a fourth order band pass Butterworth filter with parameters optimized by evaluating the spectral analysis of the blast waves (pass band 5–50,000 Hz).

After blast exposure, the holder was removed from the shock tube and the animal was inspected for injury. Genteal lubricant eye drops (Alcon, Hunenberg, Switzerland) were applied immediately after blast and at 45- to 60-minute intervals until recovery of normal blinking. This ensured eyes remained adequately hydrated during the recovery period to avoid the development of dryness and increased corneal opacity. Animals were kept on warming pads and monitored until recovery from anesthesia, at which time they were returned to cages. Animals were kept in standard day–night cycles and provided with food and water ad libitum.

Post-Blast Assessment Timeline

Control and blast-exposed rats survived 1 day, and 1, 4, or 8 weeks post-blast. Baseline contrast sensitivity testing and OCT of the cornea and retina were performed 1 day before blast exposure. Assessments were repeated 1 day after blast

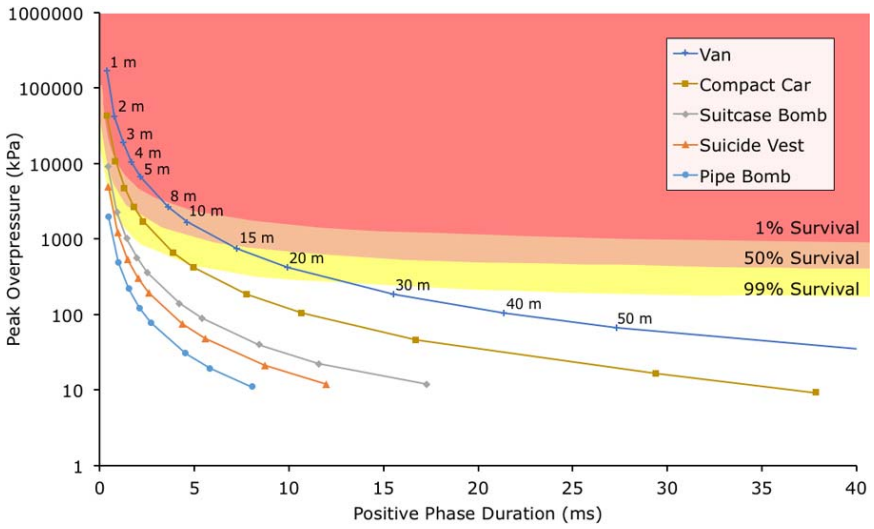

Figure 2. Chart of peak overpressure and positive phase durations for a range of explosive sources (*individual lines*) at different standoff distances (*dots*). The present study had an average ± SD blast overpressure and duration of 228 ± 28 kPa and 7.1 ± 0.6 ms, respectively. The data were calculated based on explosive magnitudes from the US Army National Ground Intelligence Center[15] and shockwave equations from Alonso et al.[16]

exposure, and then weekly until euthanization at time points required for histology and vitreous protein analysis (Fig. 3). Rats were euthanized by overdose of inhaled isoflurane and transcardially perfused with PBS and formalin. Eyes were extracted for histology ($n_{control} = 18$, $n_{blast} = 22$) or vitreous biomarker studies ($n_{control} = 12$, $n_{blast} = 20$).

Contrast Sensitivity. Visual ability was assessed by contrast thresholding with an optokinetic nystagmus (OKN) test system. The system was designed and built in-house based on similar testing apparati,[17–19] and was comprised of four LCD displays surrounding a transparent animal enclosure (Fig. 4A). A closed-circuit video camera provided visualization of the animal during stimulus tracking. The monitors displayed sinusoidal drift gratings rotated clockwise or counterclockwise around the animal enclosure driven via a custom MATLAB (Mathworks, Natick, MA, USA) code using the Psychophysics Toolbox extensions.[17,20] The drift speed (1.5 Hz) and bar spacing (0.136 rad/cycle) were held constant throughout the test, while the contrast of the grating was varied in 20% increments using a two-down, one-up staircase algorithm.[21–23]

The screens displayed a neutral gray background and the animal was placed in the center of the OKN testing platform. A wait period of approximately 5 minutes was allowed for the animal to acclimate to the test environment. The contrast grating was initiated and the test continued until a total of six contrast reversals (down–up or up–down) were recorded (Fig. 4B). The contrast change between trials was cut in half after three reversals (halfway through the test) to hone in more accurately on a threshold. The final three reversals were averaged to define the contrast threshold. To avoid interoperator bias, all behavior testing was performed by one person.

Optical Coherence Tomography. Retinal and corneal thicknesses were measured using an Envisu R220 Spectral Domain OCT (Bioptigen, Durham, NC, USA). Rats were anesthetized with 4% isoflurane, and pupils dilated with 0.5% tropicamide for 3 to 5 minutes before imaging. The anesthetized rats were placed on the test bed and imaged using the Bioptigen rat retina lens. Retinal images were captured in a 2.6 × 2.6 mm field of view, with 1000 A-scans/B-scan and 100 total B-scans. The Bioptigen telecentric lens was used to image the cornea using the same A- and B-scan parameters over a 4 × 4 mm field of view. OCT imaging was performed in right and left eyes.

Stromal, epithelial, and overall corneal thicknesses were extracted from the corneal images by measuring the thickest point of each layer using digital calipers (Fig. 5A). Overall retinal thickness and RPE evaluations were performed by manually selecting a total of 40 edge sets per OCT image stack, with four measurements taken on each of 10 B-scans spaced throughout the stack. The retinal nerve fiber layer/ganglion cell layer (NFL/GCL) thickness measurements were generated using a custom MATLAB program that calculated the layer edges in every column (A-scan) across each B-scan (green in Fig. 5B). The optic nerve region was omitted from the measurement, as were blood vessel regions (red in Fig. 5B).

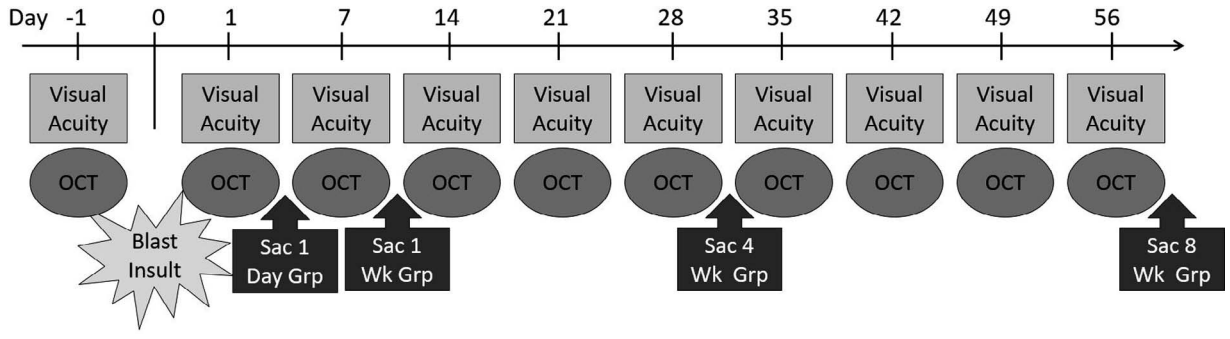

Figure 3. Experimental timeline of blast exposure, testing, and study endpoints.

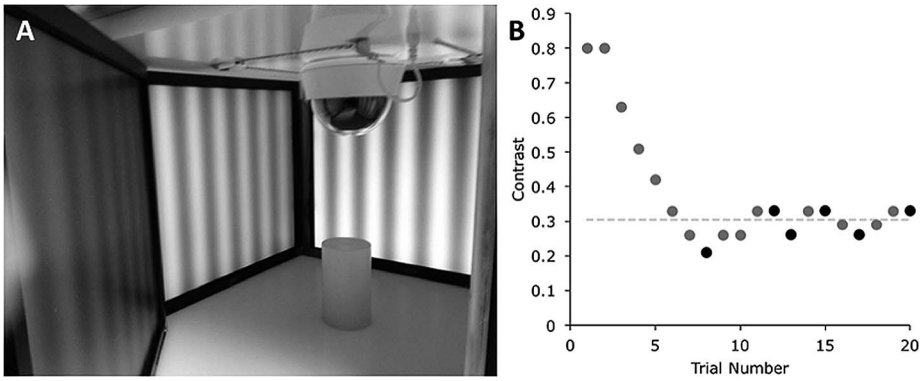

FIGURE 4. (**A**) Behavior apparatus showing drift grating on external monitors and overhead camera for tracking animal response. (**B**) Sample test result. Each *light dot* represents a single stimulus. *Dark dots* indicate the six reversals of contrast trending direction. The *line* is the calculated contrast sensitivity threshold based on the average of the three final reversals.

Thickness measurements were divided into eight radial quadrants around the optic nerve, with four central and four peripheral sections as shown in Figure 5C. Retinal image quality varied and was highly dependent on corneal opacity and thickness. At time points with severe corneal swelling and/or opacity, retinal imaging was not possible and no retinal thickness was calculated.

Ocular Histology

Eyes were stored in 4% formalin or EZ-Fix (Excalibur Pathology, Norman, OK, USA) and then sectioned (5 μm thickness) at five transverse levels. Sections were stained with hematoxylin and eosin (H&E) and TUNEL, and then examined for injury by a veterinary ocular pathologist masked to the blast exposures. Cell density in the corneal endothelium was calculated from the H&E-stained images by dividing the number of cells by the total endothelial length using a custom MATLAB image processing code.

Vitreous Protein Analysis

Eyes were eviscerated and the vitreous and lens removed. The vitreous was isolated by centrifuge and diluted with PBS (50:100 μL). The diluted sample then was separated into three equal tubes for quantification of Neurofilament Heavy Chain (NfH) and inflammatory cytokines.

Microtiter plates were coated overnight at 4°C with 100 μL capture antibody, SMI35. The plates were washed three times for 10 minutes using a barbitone buffer containing 0.1% BSA, and 0.05% Tween 20. After washing, 250 μL barbitone block with 1% BSA was added to each well and the plate was incubated at room temperature (RT) for 1 hour. After another wash cycle, 50 μL sample, standard, or negative control was added to each well of the plate in triplicate. After 1 hour incubation at RT, the wash processes were repeated. After washing, 100 μL secondary antibody was added to each well of the plate and incubated for 1 hour at RT. Following a third wash cycle, 100 μL horseradish peroxidase (HRP)–labeled swine anti-rabbit antibody was added to the plates and incubated for 1 hour at RT. After a final wash, 100 μL TMB substrate was added and incubated for 20 minutes in a dark room. The reaction was stopped by adding 50 μL 1 M HCL. The absorbance was read using an ELISA plate reader (Synergy HT Multi-Mode Microplate Reader; BioTek, Winooski, VT, USA) at 450 nm with 750 nm reference wavelength.

Quantification of inflammatory cytokines was performed using a commercially available array (RayBio Rat Cytokine

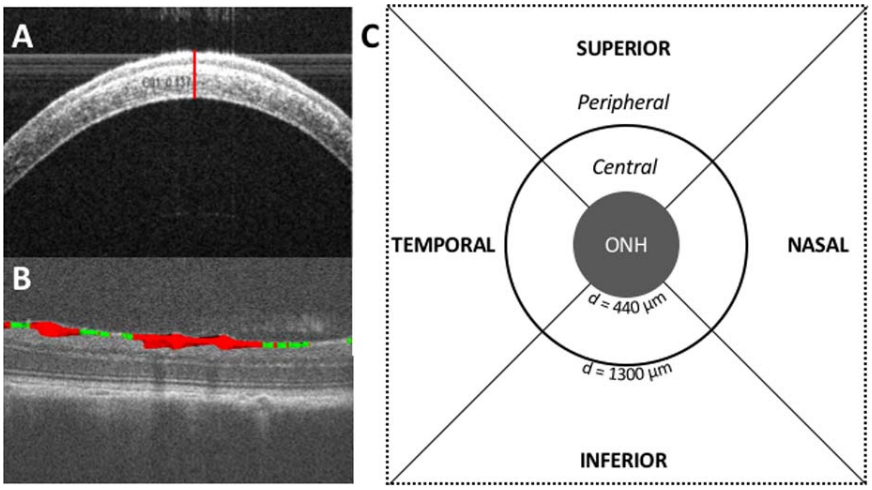

FIGURE 5. (**A**) Control corneal image illustrating how digital calipers were used to measure the overall thickness. (**B**) Retinal image with NFL/GCL thickness highlighted (*green*) and blood vessel regions (*red*) excluded. (**C**) Region breakdown for analysis of retinal thickness. The optic nerve head (ONH) was used to center each image, and then was omitted from the thickness analysis.

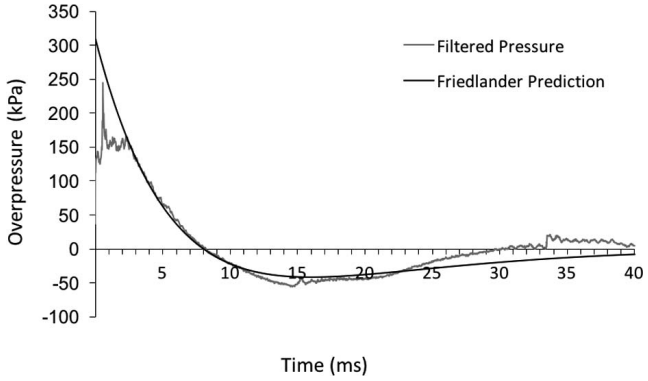

FIGURE 6. Overpressure generated by the shock tube compared to an idealized Friedlander waveform.

Antibody Array G). These arrays test for 19 cytokines. including VEGF, LIX, and TNF-α, in triplicate with positive and negative controls. Arrays were processed according to the manufacturer's instructions, and the intensities read using a GENEPIX 4000A microarray scanner at an excitation frequency of 532 nm. Cytokine quantification was normalized against the positive controls.

IOP Measurement

In a separate set of animals ($n = 10$), fiberoptic pressure sensors (FISO FOP-LS-2FR-30, Quebec, Canada) were placed in each eye to measure the IOP in the directly- and indirectly-exposed eyes during a blast. Animals were anesthetized as described previously, but dexmedetomidine dosage was increased to 0.25 mg/kg. The lateral commissure was clamped with a hemostat for several seconds to limit bleeding, and then cut to gain access to the posterior half of the eye. The IOP transducers were prethreaded through surgical tubing and into the midsection of an 18-gauge hypodermic needle. Tweezers were used to grasp the conjunctiva near the commissure and rotate the eye in the medial direction. The needle containing the pressure transducer was inserted through the posterior sclera and positioned into the central vitreous chamber. The conjunctiva was released and the eye allowed to rotate back gently into its natural position. Skin sutures and cyanoacrylate adhesive secured the surgical tubing to the back of the rat to limit sensor cable motion during animal positioning and blast wave exposure. The procedure was repeated for the other eye. Rats were secured in the blast tube and exposed to blast pressure magnitudes as described previously. After blast exposure, animals were euthanized and sensors removed.

The fiber optic transducers were connected to the FISO signal conditioner with a sampling frequency of 15 kHz. Data from the signal conditioner were recorded with the same acquisition system as the tube-mounted pressure sensors. The IOP data were not filtered because the sample rate from these sensors was below the cutoff frequency used for the tube pressure sensors. IOP data traces were analyzed in MATLAB to record peak pressure, rise time, initial slope, positive, negative, and net impulse for each curve.

Data Analysis

Statistical analyses were performed using R (RStudio, Inc., Boston, MA, USA). To determine if blast-exposed or control animals significantly differed from baseline at any time point, contrast sensitivity at each time point was compared to the animal's baseline score using a 2-tailed matched pair Student's *t*-test, with the Bonferroni correction for multiple comparisons.

TABLE 1. Summary of Blast Characteristics From Animal Blast Exposures

Blast Parameter	Av. ± SD
Peak overpressure, kPa	228.49 ± 28.49
Peak negative pressure, kPa	−50.81 ± 6.62
Positive phase duration, ms	7.06 ± 0.64
Negative phase duration, ms	21.62 ± 2.04
Positive phase impulse, Pa-s	680.51 ± 66.88
Negative phase impulse, Pa-s	571.58 ± 77.91
Net impulse, Pa-s	1250.71 ± 102.01

Then, at each time point, the control group was compared statistically to the blast-exposed group with a 2-tailed Student's *t*-test. All analyses were performed using $\alpha = 0.05$ as the confidence level. The same statistical comparisons were used to assess differences from baseline and from time-matched controls for corneal and retinal thicknesses, endothelial cell density, and vitreal protein expression. Statistical comparison between the pressure waveform characteristics in the tube and in the eyes was performed using a 1-way matched pair ANOVA with the same type I error ($\alpha = 0.05$). Histology findings were evaluated statistically using χ^2 test to evaluate differences between blast and control groups and between left and right eyes.

RESULTS

The shock tube delivered consistent blast levels with a Friedlander waveform shape, indicating accurate recreation of open field blast (Fig. 6). Blast waveform characteristics are summarized in Table 1. Four blast-exposed animals (7.4%) experienced apnea immediately after blast, two of which did not recover. One animal recovered following manual chest compressions. A second animal experienced apnea 30 seconds after removal from the shock tube (approximately 1 minute from blast exposure) and did not recover. A single animal died 15 minutes after blast, despite showing no immediate signs of injury directly after the blast exposure. The overall mortality rate for all blast-exposed animals was 7.4% (4/54). Incidental minor injuries included nosebleed (2/54) and tongue bite (2/54).

In an initial subset of animals ($n = 4$), corneas were examined using fluorescein dye roughly 5 minutes after blast exposure. No abrasions or abnormalities were found, verifying that no secondary contact injuries were inflicted during the blast due to microparticles of the burst membrane traveling down the tube. Review of high-speed recordings of blast exposure further confirmed there were no shrapnel injuries.

Contrast Sensitivity

Blast-exposed animals experienced a measurable and sustained visual system impairment following injury. Contrast thresholds significantly increased in blast-exposed animals compared to their baseline values at 1 day, and 2, 5, 7, and 8 weeks after blast exposure ($P < 0.05$). This increase began the day after exposure and persisted until the end of the study at 8 weeks (Fig. 7). Contrast sensitivity in blast-exposed animals was significantly worse than in control animals at all time points after blast exposure ($P < 0.05$). Contrast thresholds in control animals improved from baseline values by week 1 and then remained stable, with statistically significant improvements from baseline at 3 and 7 weeks after sham blast ($P < 0.05$). This may have been caused by increased comfort with the test enclosure and handling procedures. In a more relaxed state,

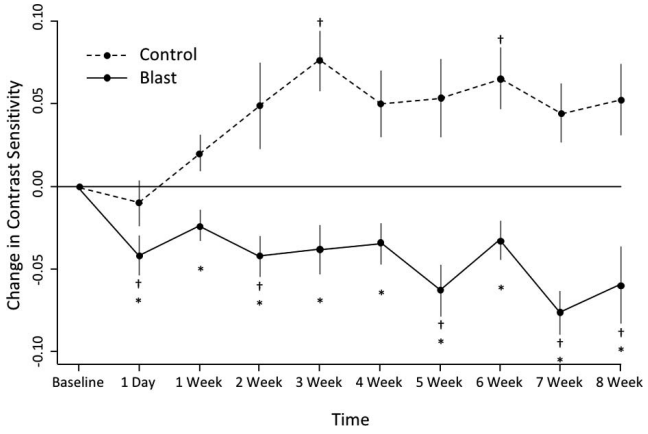

FIGURE 7. Contrast sensitivity changes in blast-exposed and control animals over the course of 8 weeks. *Error bars*: standard error of the mean. *Significant differences between control and blast-exposed animals at each time point ($P < 0.05$). †Significant changes relative to baseline visual ability (Bonferroni-adjusted $P < 0.05$).

the animals tended to increase focus on the screens surrounding them.

Optical Coherence Tomography

Significant structural changes in blast-exposed eyes were found with OCT imaging. In general, the changes were delayed temporally from the initial blast exposure by at least 2 weeks. The changes were more substantial in the directly exposed right eye compared to the indirectly exposed left eye, but both eyes experienced significant corneal changes ($P < 0.05$).

Cornea. Stromal thickness in the indirectly exposed left eye at 1 week after blast significantly increased by 57 ± 59 μm ($P < 0.0001$) and resolved to baseline values by the following week (Fig. 8A). A similar increase of 57 ± 53 μm was found at 1 week after blast in the directly exposed right eye, but this change was not significant until 2 weeks after blast exposure due to increased variance in the baseline thickness of the right compared to the left eyes. Between 2 and 5 weeks, 42% of the animals surviving at least 1 week after blast had significant stromal thickening ($P < 0.033$). The remaining 58% of the animals did not experience corneal swelling. The swelling, as measured by a change in thickness from baseline, reached maximum increases of 136 ± 198 μm by week 5. At week 6, left and right stromal thicknesses returned to near-baseline values, but the right eye was still 40 ± 23 μm thicker than the original baseline measurement. Epithelial thickness of directly exposed right eyes significantly thickened by 107.3 ± 135 μm at 6 weeks after blast (Fig. 8B, $P < 0.05$). The epithelium decreased to 25 ± 32 μm above baseline thickness by 8 weeks after blast exposure. No significant changes were found in control animals for either the stroma or epithelium.

Although stromal and epithelial swelling mostly resolved by the end of the study, persistent damage was observed in the form of stromal scarring (Fig. 9). In total, half of the animals surviving to 8 weeks after blast had corneal thickening at 3 to 5 weeks, and all animals with corneal thickening exhibited stromal scarring at the final study time point. A single control animal (1/38) had corneal thickening at 3 to 5 weeks; and later experienced stromal scarring at 8 weeks. This injury was thought to be due to an altercation with another animal in the cage. Of note, this animal was assigned randomly to the vitreal analysis group, so no further histology was performed.

Retina. Retinal thickness changes were not as conclusive as the corneal findings. Statistical analysis of overall thickness found that there was significant thickening of the retina at 7 weeks in the right eye of blast-exposed animals when regions were averaged across the central ring (Fig. 10, $P = 0.02$). A similar increase was seen in the indirectly exposed eye, but it was not statistically significant. There were no other significant findings in other regions or time points. There were no significant thickness changes from baseline in the RPE layer in any group or at any time point. The analysis of the combined NFL/GCL likewise found no significant thickness changes from baseline.

Ocular Histology

Corneal histology showed transient injury in control animals at 1 day and 1 week after blast, limited to infiltration of inflammatory cells into the stroma ($n = 10/36$) and epithelial bullae ($n = 6/36$). Later time points in control animals had no significant injury findings in either the cornea or lens. In contrast, blast-exposed animals had positive histology after 1 week. The most common corneal injury findings in blast-exposed animals were epithelial bullae ($n = 20/57$), stromal inflammation ($n = 18/57$), stromal vascularization ($n = 9/57$), and subepithelial scarring ($n = 7/57$). The prevalence of injury in blast-exposed animals was significantly greater than control animals for every injury classification ($P < 0.05$), with the exception of stromal inflammation. The only significant difference between left and right eyes was a higher incidence of epithelial ingrowth at bullae in the left eye of blast-exposed animals compared to the right ($P = 0.0058$). These findings are summarized in Table 2 and correlate well with the timeline of corneal damage seen in the OCT (Figs. 8, 9). In 9/57 (16%) blast-exposed eyes, superficial damage to lens was found that indicated cataract development, such as lens fiber swelling, liquefaction, and formation of morgagnian globules. No microscopic retinal injuries were detected in the stained tissues. Figure 11 displays representative images of the common histological presentations.

The blast-exposed animals had significantly higher ($P < 0.0001$) endothelial cell density than the control animals in the left (0.0236 ± 0.0042 cells/pixel) and right (0.0226 ± 0.0034 cells/pixel) eyes. Within the blast-exposed animals, cell density was significantly higher at 1 and 4 weeks compared to 1 day and 8 weeks after blast. The endothelial cell density of the control animals did not change significantly between time points or between left (0.0202 ± 0.0031 cells/pixel) and right (0.0201 ± 0.0025 cells/pixel) eyes.

Vitreal Protein Analysis

The left and right eyes of blast-exposed animals exhibited increased concentrations of NfH 1 day after blast exposure ($P < 0.05$, Fig. 12B). Between 4 and 8 weeks, NfH concentration decreased significantly but still was elevated with respect to controls. Inflammatory cytokines generally exhibited a transient increase in expression 1 week after blast that resolved by the end of the study (Fig. 12A). Beta nerve growth factor (β-NGF), shown to promote corneal healing,[24] significantly increased in blast-exposed eyes between 1 day and 4 weeks ($P < 0.05$), and returned to control values by 8 weeks (Fig. 12C). Ciliary neurotrophic factor (CNTF), typically upregulated upon injury to neural tissue, significantly increased in blast-exposed animals at 8 weeks after blast ($P < 0.05$, Fig. 12D).

Intraocular Pressure

IOP was measured successfully in right and left eyes in 8 of the 10 animals. During initial blast wave contact with each eye,

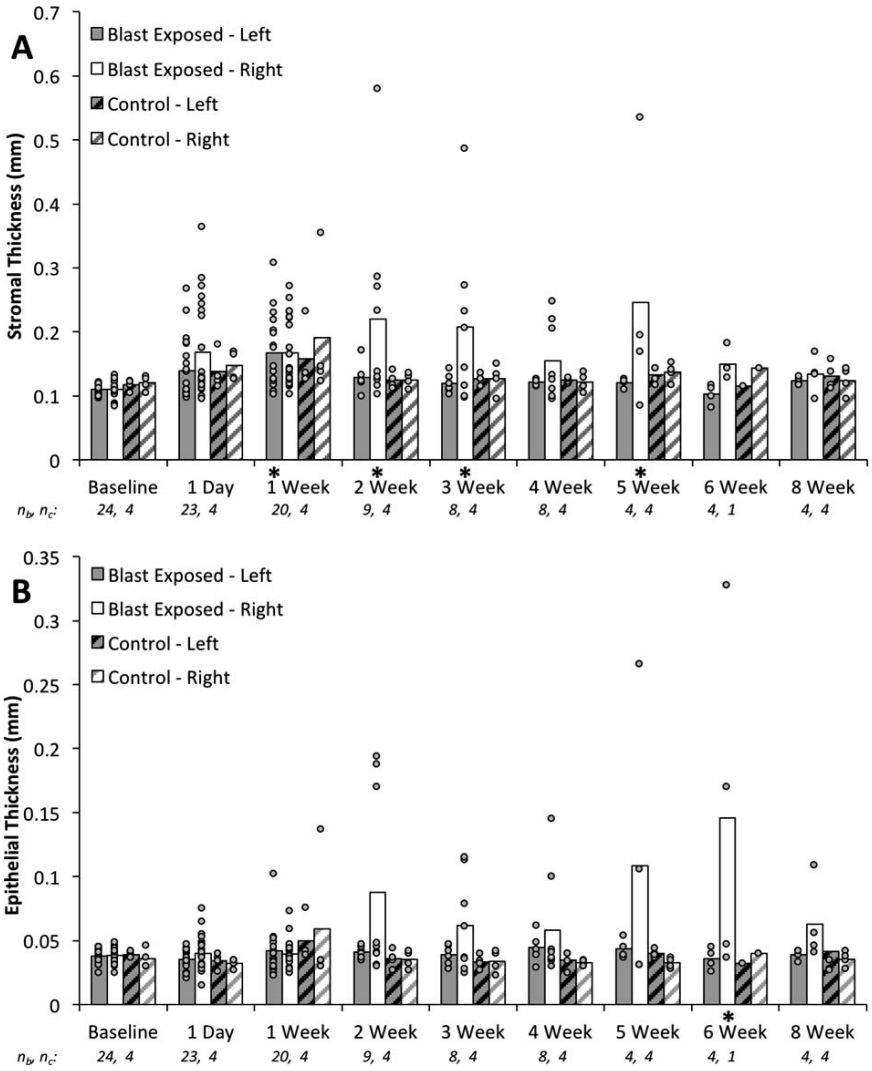

Figure 8. Thickness of the corneal stroma (**A**) and epithelium (**B**) as a function of time. *Columns* represent average thickness with individual measurements overlaid. The directly blast-exposed right eyes exhibited stromal (1 day–5 weeks) and epithelial (2–6 weeks) swelling. The data were binary, meaning there was a group of animals that experienced significant thickness changes while another group remained near baseline thickness. Significant (Bonferroni adjusted $P < 0.05$) changes from baseline are noted by an asterisk (*) below the column. Sample sizes for blast and control animals are indicated by n_b and n_c, respectively.

IOP closely mimicked the general Friedlander waveform. However, after initial contact, IOP readings became erratic. This could have been caused by sensor movement within the eye, contact between the ocular lens and sensor tip, and/or wave reflection inside the eye. Based on the initial 5 ms of the pressure waveform it was observed that peak pressure in the directly exposed eye (231.9 ± 40.9 kPa) matched the tube pressure (240.3 ± 39.0 kPa) measured 2 cm in front of the animal within 0.1% with a 0.6775 ms delay (Fig. 13). One kPa is equivalent to 7.5 mm Hg, so IOP effectively increased from normal IOP (12–22 mm Hg) to 1739 ± 307 mm Hg during the blast. The IOP peak pressure in the indirectly exposed eye was 30% lower than in the directly exposed eye, but this decrease was not statistically significant. Pressurization rate decreased significantly by 61% as the blast wave traveled from the tube into the directly exposed right eye and decreased significantly by another 60% as the wave traveled through the head into the indirectly exposed left eye ($P < 0.01$). The positive phase impulse in the tube and right eye did not differ significantly, but the tube was significantly higher by 32% compared to the left eye ($P < 0.05$), and the negative phase impulse magnitude was 35% lower in the right eye than in the tube ($P < 0.01$). The net impulses recorded in the tube, and left and right eyes did not differ significantly.

Discussion

To improve diagnosis and treatment strategies for blast ocular trauma, it is important to understand the types of injuries that occur as well as the timelines for injury development. The objective of this study was to identify ocular blast exposure sequelae up to 8 weeks. To achieve this objective, we experimentally reproduced open field primary blast ocular trauma in a rat model, and quantified ocular damage with OCT, visual function, histology, and vitreous protein analyses for a 2-month period. Side-on blast was used in this study to limit the exposed area to the head and eye, while protecting the trunk and specifically the lungs of the animal. Importantly, it also allowed a comparison between directly- and indirectly-exposed eyes. In vivo IOP was measured during some blast exposures to quantify the difference between directly- and indirectly-

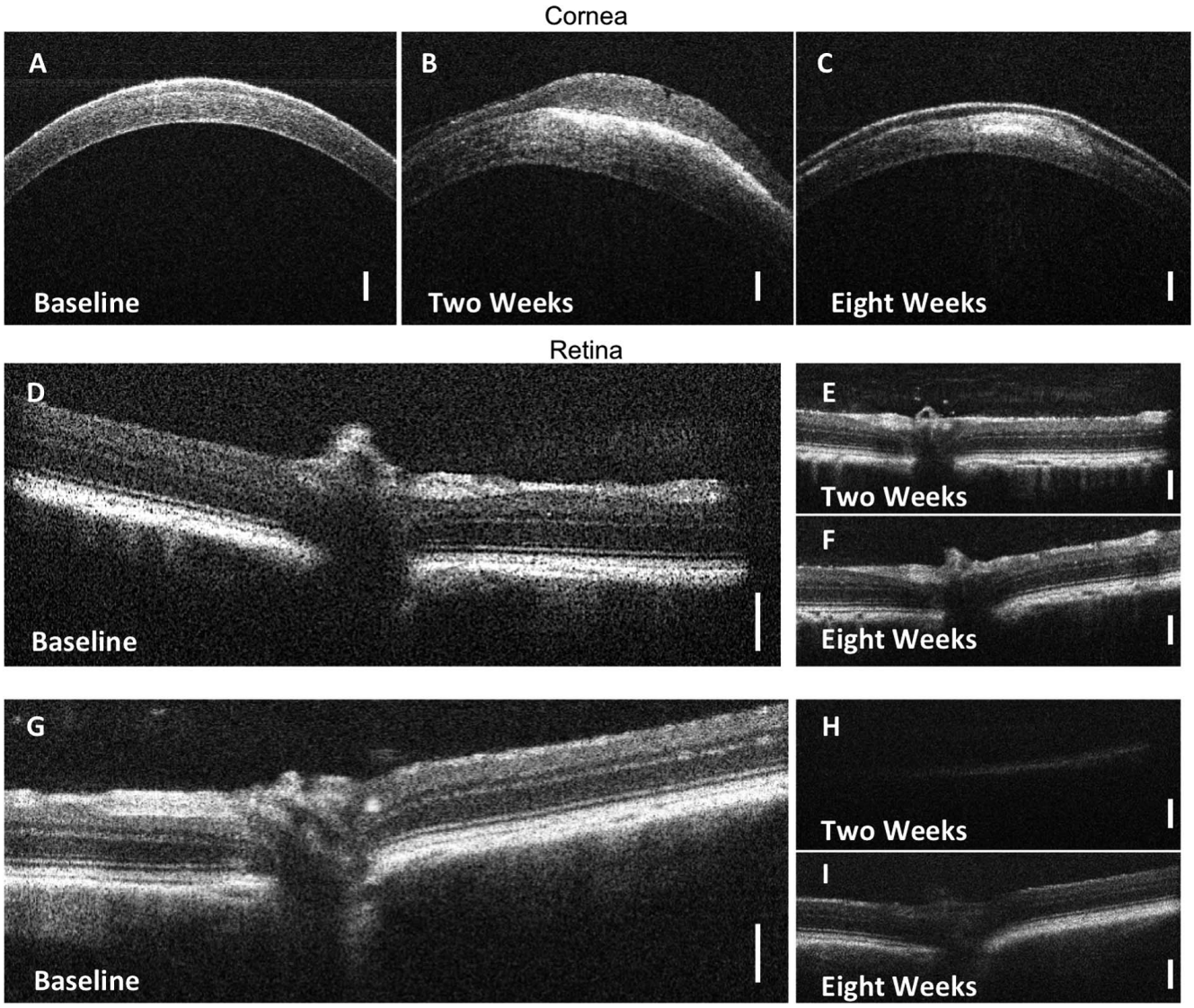

FIGURE 9. *Top*: Progression of corneal damage in the right eye of a single animal. (**A**) All animals at baseline exhibited healthy corneas. (**B**) Substantial swelling occurred 2 weeks after blast exposure. (**C**) Thickening decreased 8 weeks after blast exposure but stromal scarring remained. *Bottom*: (**D–F**) Progression of retinal imaging in the right eye in a blast-exposed animal without corneal damage. (**G**) Baseline image in blast-exposed animal that later developed corneal damage shows healthy retina and optic nerve with clear discrimination of retinal layers. (**H**) At 2 weeks, corneal swelling reduced image quality severely and no retinal thickness measurements could be made. (**I**) By 8 weeks, the image quality improved and thickness measurements were recorded. The animal in (**A–C**) is different than the animal in (**G–I**). *Scale bars*: 100 μm.

exposed eyes. Blast exposure resulted in lasting visual and anatomical defects in a significant number of animals. Each injury had its own unique temporal time course, which is discussed in detail in the following subsections.

Decreased Contrast Sensitivity was Immediate and Sustained

Contrast sensitivity deficits were immediate and did not improve over 2 months subsequent to blast exposure. The deficit appeared only in the blast-exposed animals. The presence of delayed visual injury has been reported clinically in blast-exposed soldiers[13,25] as well as by previous experimental studies.[26] However, the diminished visual function in animal studies has been linked commonly to posterior pole eye injuries in the retina, optic nerve, or traumatic brain injury (TBI). In this study, we did not evaluate brain injury, optic nerve damage, or retinal function, so it is unknown what specifically caused the decreased contrast sensitivity. In a small subset of animals ($n = 9$), we evaluated each eye independently and found worse contrast thresholds in the right (directly exposed) compared to the left eyes. This suggests that the problem may be related to optic nerve, corneal, or retinal damage rather than brain injury.

In our study, no significant changes were found in retinal thickness. Mohan et al.[14] also did not find significant retinal thinning until 3 months after injury. However, other researchers have reported retinal thinning and degeneration at 2 to 4 weeks after exposure to similar peak blast pressures.[4,27] Differences in species, blast device, and study design likely contributed to the conflicting results. Although we did not detect retinal changes via OCT, NfH levels were increased immediately in blast-exposed animals and CNTF increased significantly at 8 weeks after blast exposure. NfH is released from degenerating retinal ganglion cells and axons into the vitreous[28] and CNTF is upregulated in response to neural

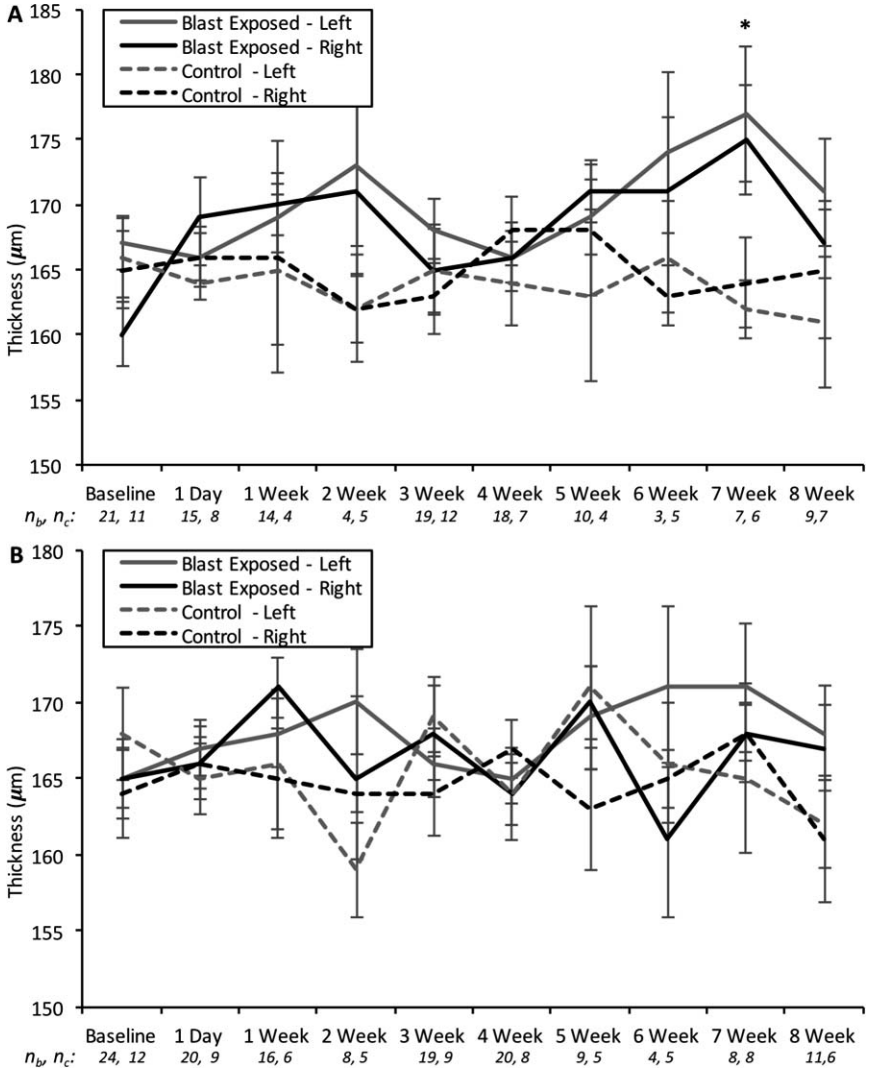

Figure 10. (**A**) Central and (**B**) peripheral retinal thickness for direct (right eye) and indirect (left eye) blast exposure. There was significant ($P < 0.05$) thickening at 7 weeks compared to baseline in the central region of the right eye. *Error bars*: standard error. Sample sizes for blast and control animals indicated by n_b and n_c, respectively.

Table 2. Summary of Histology Findings

	Control										Blast									
	Total		1 Day		1 Wk		4 Wk		8 Wk		Total		1 Day		1 Wk		4 Wk		8 Wk	
	L	R	L	R	L	R	L	R	L	R	L	R	L	R	L	R	L	R	L	R
n	18	18	6	6	6	6	3	3	3	3	28	29	5	5	8	8	9	9	6	7
Cornea																				
Epithelial bullae	17%	17%	33%	33%	17%	17%	0%	0%	0%	0%	43%	29%	0%	0%	63%	75%	44%	22%	50%	0%
Inflammatory cells in stroma	22%	33%	50%	67%	17%	33%	0%	0%	0%	0%	32%	32%	0%	0%	63%	63%	22%	33%	33%	14%
Epithelial ingrowth at bullae	0%	0%	0%	0%	0%	0%	0%	0%	0%	0%	18%	0%	0%	0%	13%	0%	33%	0%	17%	0%
Stromal vascularization	0%	0%	0%	0%	0%	0%	0%	0%	0%	0%	21%	11%	0%	0%	13%	13%	33%	11%	33%	14%
Lens																				
Subepithelial scarring	0%	0%	0%	0%	0%	0%	0%	0%	0%	0%	11%	14%	0%	0%	0%	13%	11%	11%	33%	29%
Epithelial vacuolization/drop out	0%	0%	0%	0%	0%	0%	0%	0%	0%	0%	18%	14%	0%	0%	25%	13%	33%	33%	0%	0%
Fiber cell swelling/membranolysis	0%	0%	0%	0%	0%	0%	0%	0%	0%	0%	18%	14%	0%	0%	25%	13%	33%	22%	0%	14%

Except for stromal inflammation, all injury findings were significantly more prevalent in blast than control animals ($P < 0.05$).

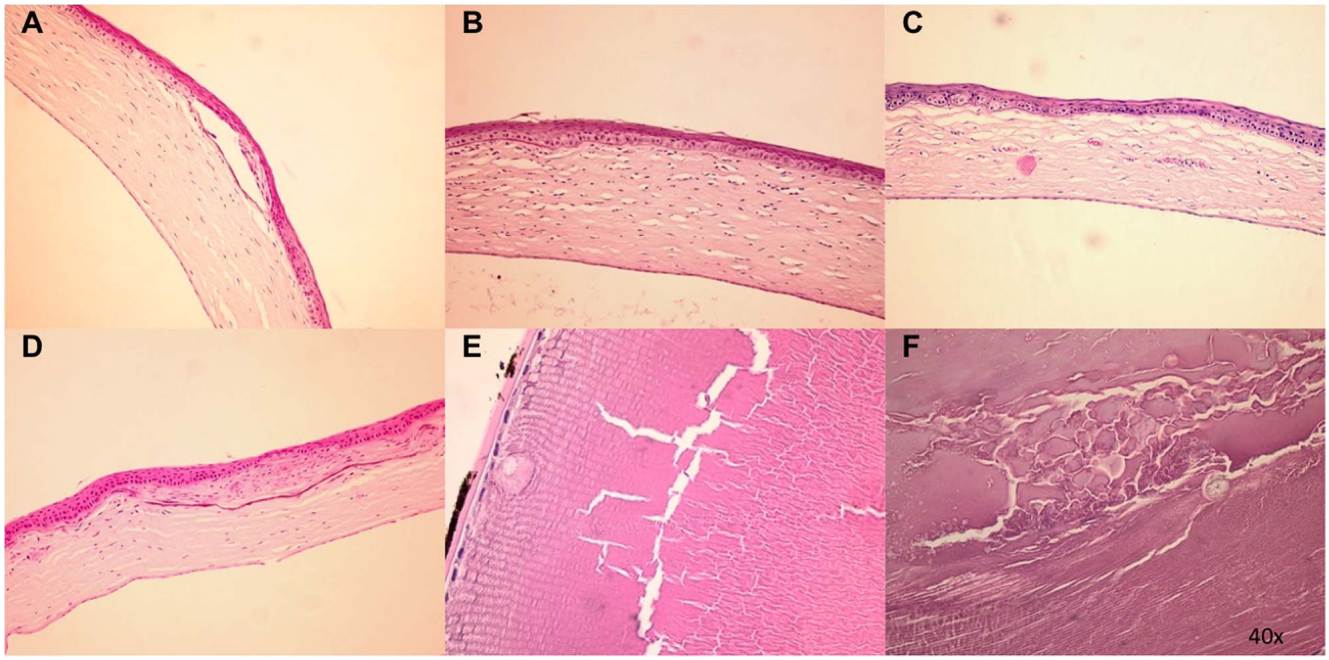

FIGURE 11. Representative images (×20 magnification) of common histology injury presentations: (**A**) Subepithelial bullae with epithelial ingrowth. (**B**) Infiltration of inflammatory cells into stroma. (**C**) Stromal neovascularization with accompanying stromal inflammation. (**D**) Subepithelial scarring with disruption of basal lamina. (**E**) Lens fiber swelling. (**F**) Lens fiber liquefaction with formation of morgagnian globules.

injury.[29] Elevation of these proteins indicated possible retinal damage that was not detected by OCT or histology.

The lack of significant retinal findings in our study also may be attributable to large variability between animals or impedance of corneal damage on image analysis. An increase in corneal opacity occurs during corneal swelling and likely decreased the effective resolution of the retinal OCT images. At some time points, we were unable to visualize the retina at all due to severe corneal damage (Fig. 9H). In these cases, retinal damage may have been present, but not captured by the OCT

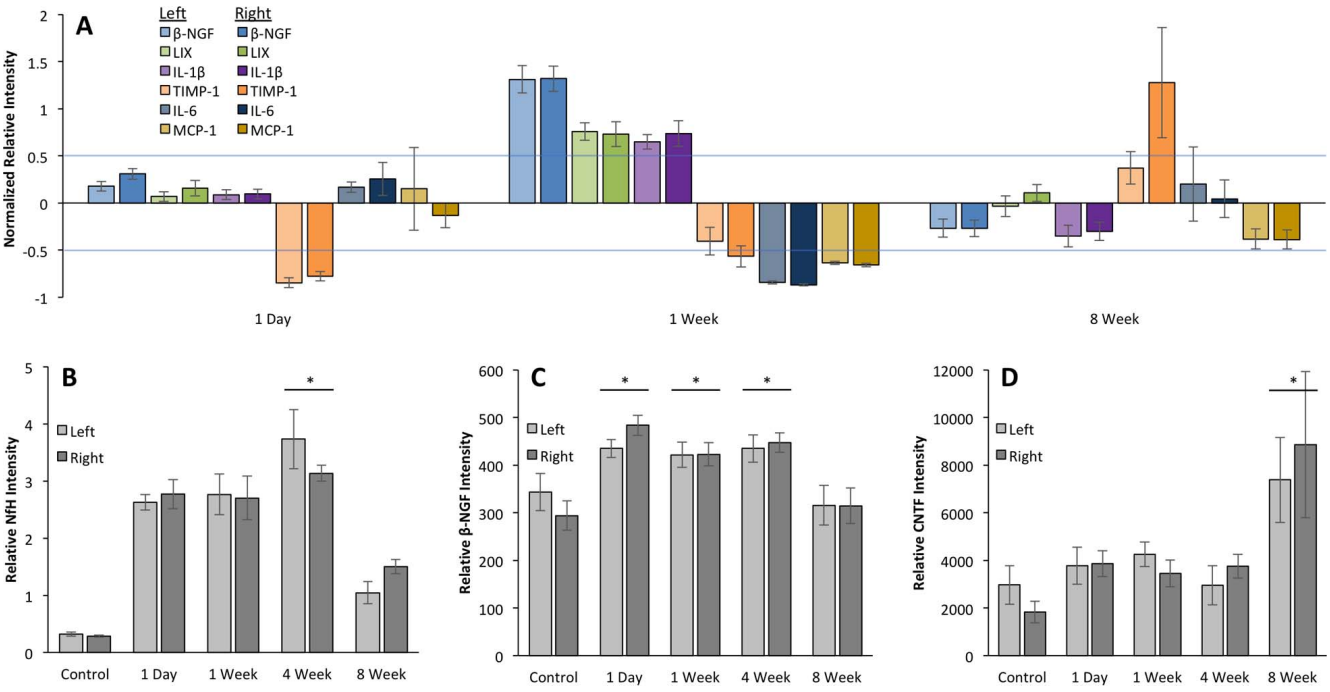

FIGURE 12. Results of vitreous protein quantications. (**A**) Selected cytokines normalized by relative intensities in time-matched control animals. Both eyes had a general increase in response 1 week after injury, but returned to control levels by 8 weeks. *Lines* indicate a 50% increase or decrease in intensity. (**B**) NfH was signicantly greater in injured animals compared to control animals for all time points. At 8 weeks, NfH signicantly decreased toward control levels. (**C**) β-NGF significantly increased from 1 day to 4 weeks and then returned to baseline. (**D**) CNTF was significantly elevated at 8 weeks after injury compared to controls. $^*P < 0.05$

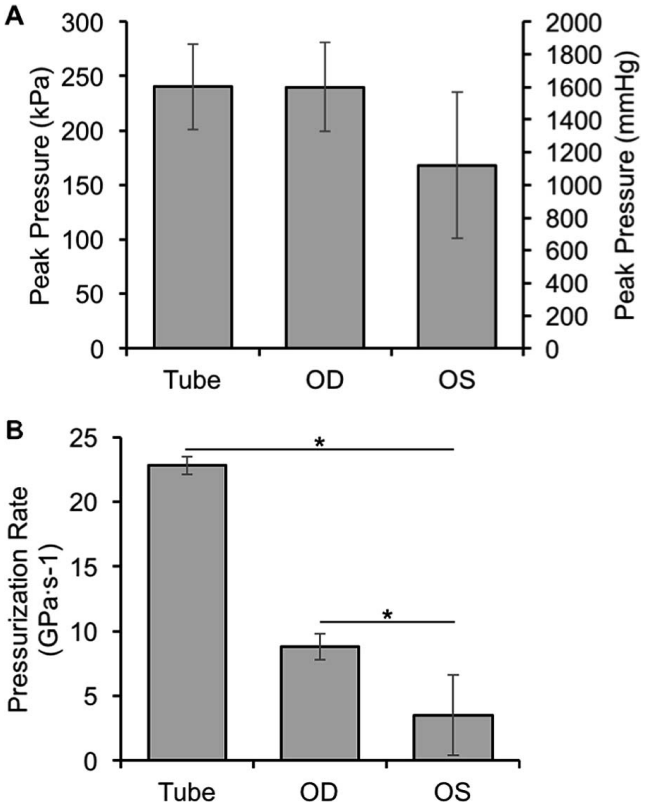

FIGURE 13. Average peak pressure and pressurization rate measured in the shock tube compared to IOP measured in the left and right eye of the animals. There was no significant difference between the peak pressure of the tube and the directly-exposed right eye. The peak pressure in the left eye was reduced by 30%, but this was not significant. The pressurization rate was significantly lower in the right eye than in the shock tube and significantly lower in the left than the right eyes ($^*P < 0.01$).

imaging. Future studies using this blast model could address this limitation by including electroretinography (ERG) or visual evoked potentials (VEP) at each testing time point to assess retinal function in addition to structural changes. Corneal swelling also could contribute to the visual dysfunction seen in our study, but thickening in the cornea peaked at 3 to 5 weeks after blast exposure and did not completely explain the immediate visual dysfunction. Further, decreases in contrast sensitivity were noted in animals without corneal swelling. The initial decrease in contrast sensitivity at the 1 day time point appeared to present in both the control and blast-exposed animals. Some of this decrease may be due to the stress of the anesthesia procedure or residual effects of anesthesia. Additionally, some of the visual deficits occurring before corneal swelling may be attributed to corneal opacity, which preceded the measurable swelling at later time points.

Corneal Swelling/Scarring was Delayed and Temporally Complex

The temporal progression of corneal damage was an interesting finding in this study. The majority of corneal injuries reported in previous blast animal models have been short duration edema and abrasion. One exception to this is a single animal experiencing corneal scarring at 4 weeks after a 162.7 kPa blast in the study of Hines-Beard et al.[4] In our study, epithelial swelling occurred at 2 weeks, diminished, and then experienced a resurgence of significant swelling at 6 weeks. This resurgence was due to the stromal swelling during weeks 2 through 5. The delay between blast exposure and subsequent corneal swelling may be due to damage to the corneal endothelium, which would allow increased uptake of water from the aqueous into the cornea. We found increased epithelial cell density at 1 and 4 weeks after blast exposure, which suggested cellular recruitment in response to dysfunction. Corneal scarring always followed stromal swelling and was present by 8 weeks. Corneal thickness trended toward baseline values by the end of the study, but there was a remaining thickening of 10% (20 μm) in the stroma of both eyes suggesting some residual edema. This edema, coupled with the scarring, likely contributed to the poor overall visual ability in the animals at these later time points.

The majority of corneal injury was seen in the directly exposed eye, but the directly- and indirectly-exposed eyes were damaged. At 1 week after blast, both eyes were thickened with respect to baseline by 57 μm. Only the indirectly exposed eye reached statistical significance due to the higher variance in the directly exposed eye. Potential sources for the increased variability could be slight changes in head angle, eyelid position, and head strap tightness. This variance hindered statistical power at the later time points due to the decreased sample sizes resulting from histological euthanization.

Review of H&E- and TUNEL-stained eyes revealed corneal epitheliopathy in blast-exposed animals (Table 2). Of note, some number of control animals had epithelial bullae and stromal inflammatory infiltration, despite no exposure to a blast wave. It is likely that the bullae at this time point were caused by artifact due to tissue processing, and the stromal inflammation a response to anesthesia or procedural effects. However, subepithelial scarring was found only in blast-exposed eyes and peaked at 8 weeks after blast. This correlated well with the timeline of corneal damage seen in OCT imaging. Similarly, neovascularization was detected only in blast-exposed animals, and further confirms the activation of corneal inflammation and healing processes suggested by OCT.

The delay between initial blast exposure and subsequent corneal changes suggested that targeted drug treatment may be possible in the 2-week window before symptoms develop. Biomarkers associated with inflammation, including IL-1β and LIX, were elevated between 1 day and 4 weeks after blast exposure. The timing of these elevated concentrations suggested that these markers may be associated with the corneal swelling detected between 2 and 6 weeks. LIX, in particular, has been associated previously with neutrophil infiltration to the stroma and keratitis.[30] After cytokine levels decreased, swelling resolved and scar tissue remained. Further investigation of significantly elevated vitreal proteins following blast exposure may reveal potential targets for medical intervention.

Initial concerns that the corneal damage might be due to blast fragments of the Mylar membrane were assuaged by fluorescein staining immediately after blast, which revealed no signs of abrasions. Thus, we believe that the damage truly was caused by the blast pressure wave. A cross-sectional study performed by Cockerham et al.[31] in 2014 found similar corneal injuries in blast-exposed veterans. Specifically, 25% of nonpenetrative exposures resulted in anterior pole injuries and include stromal scarring. The corneal damage in our model may be more prevalent due to the single mode of blast injury we are simulating. In combat, many soldiers experiencing comparable strength blast loading also are susceptible to other injury mechanisms. Penetrating injuries from shrapnel and flying debris injuries, in particular, may mask some of the effects of pure primary blast on the cornea. Further, protective eyewear may reduce the prevalence of corneal scarring in the clinical population.

In addition to the corneal findings, blast-exposed animals had significant lens pathology compared to controls. These

findings include epithelial cell vacuolization (33% of 4-week eyes) and lens fiber swelling or membranolysis (24% of 1- and 4-week eyes). These lens findings likely underrepresent the frequency of lens injury in our blast-exposed animals, as fixation artifacts prohibited analysis for many lens samples. Clinically, cataracts have been reported in 11% of closed-globe blast exposures,[13] and we believe that these animal model results show the early stages of cataract formation.

IOP Rapidly Increased to Applied Overpressure

Understanding IOP during and after blast is critical to understanding injury mechanisms. Measurements of in vivo IOP during blast exposure revealed that internal ophthalmic pressures were orders of magnitude above normal physiologic levels. This large increase was only for 6 ms. IOP was not tracked over the duration of 8 weeks in our study; however, other studies have shown transient significant increases in IOP by 35% in the first 24 hours after blast, followed by significant, chronic decreases in IOP.[4,6]

Internal ophthalmic pressures in directly-exposed eyes closely matched external tube measurements. Therefore, tube pressure measured 2 cm before the animal is a suitable surrogate for IOP in directly-exposed eyes. Tube pressure may not be a good surrogate for IOP in indirectly-exposed eyes, as the tube pressure was higher than in the indirectly exposed eye, although this difference was not significant. Decreases in peak pressure and pressurization rate observed in the indirectly exposed eye help account for the lower incidence of long-term stromal swelling and scarring found in left eyes. These data highlight the important role of facial structures and blast wave direction in determining risk of ocular trauma from blast.

Translation of Rodent Eye Findings to Humans

Several distinctions between rat and human eyes are important to consider when extrapolating findings in this study to a human population. First, rat eyes are placed laterally,[32] so most experimental studies can investigate directly- and indirectly-exposed eyes. Front-on blasts in humans are likely to generate some gradient between directly- and indirectly-exposed eyes due to the central facial structures. Second, the globe diameter, retinal thickness, and corneal thickness of the rat eye is roughly 20% to 40% of the human eye.[33,34] No methodology for scaling currently exists, so it is unclear how experimental blast pressure magnitudes and durations relate to military blast exposures. Third, the cornea makes up a much larger portion of the globe of the eye in the rat compared to the human. This may result in greater relative deformations of the cornea following blast exposure. Finally, the rat lens takes up proportionally greater space than the human lens. The lens is significantly stiffer than all other ocular components, so this difference may have important ramifications on the dynamic response of the eye to blast loading. Despite these distinctions, we chose rats for the development of our ocular blast model because of the availability of established methods for characterizing visual ability, the feasibility of longer-term studies, and the ability to compare findings to those of other studies in the literature. Computational modeling of the rodent and human eyes in blast may provide further insight into potential implications of species-related differences to loading.

Conclusions

Following blast exposure, contrast sensitivity significantly decreased immediately after blasts and persisted for at least 8 weeks in the rodent. Severe, delayed corneal damage may account for some of this visual deficit, but other mechanisms, such as retinal functional damage or TBI, must be responsible for more immediate visual dysfunction. These longer-term studies elucidate the temporal progression of ocular impairment, and the unique 2-week time delay of corneal swelling suggests a possible treatment window to mitigate corneal swelling and scarring after blast exposure, and potentially improve long-term visual outcomes.

Acknowledgments

The authors thank Stewart Yeoh for his assistance with high speed video of blast, as well as Lauren Lentsch and Jack Taylor for their advice on animal procedures.

Supported by the United States Army Medical Research and Material Command Award W81XWH-12-1-0243. The views, opinions, and/or findings contained in this work are those of the authors and do not necessarily reflect the views of the Department of Defense, and should not be construed as an official DoD/Army position, policy or decision unless so designated by other documentation.

Disclosure: **D.F. Shedd**, None; **N.A. Benko**, None; **J. Jones**, None; **B.E. Zaugg**, None; **R.L. Peiffer**, None; **B. Coats**, None

References

1. Gagliano DA, Lawrence MG. Presentation to the Recovering Warriors Task Force. Vision Center of Excellence, Bethesda, Maryland, United States, 2012.
2. Wong TY, Seet MB, Ang CL. Eye injuries in twentieth century warfare: a historical perspective. *Surv Ophthalmol*. 1997;41:433–459.
3. Mader TH, Carroll RD, Slade CS, George RK, Ritchey JP, Neville SP. Ocular war injuries of the Iraqi Insurgency, January-September 2004. *Ophthalmology*. 2006;113:97–104.
4. Hines-Beard J, Marchetta J, Gordon S, Chaum E, Geisert EE, Rex TS. A mouse model of ocular blast injury that induces closed globe anterior and posterior pole damage. *Exp Eye Res*. 2012;99:63–70.
5. Sundaramurthy A, Alai A, Ganpule S, Holmberg A, Plougonven E, Chandra N. Blast-induced biomechanical loading of the rat: an experimental and anatomically accurate computational blast injury model. *J Neurotrauma*. 2012;29:2352–2364.
6. Jones K, Choi JH, Sponsel WE, et al. Low-level primary blast causes acute ocular trauma in rabbits. *J Neurotrauma*. 2015.
7. Dewey J. The shape of the blast wave: studies of the Friedlander Equation. *21st International Symposium on Military Aspects of Blast and Shock*. Israel; 2010.
8. Holmberg A. *Development and Characterization of Shock Tubes for Laboratory Scale Blast Wave Simulation* [master's thesis]. Lincoln, Nebraska: University of Nebraska; 2010.
9. Zou YY, Kan EM, Lu J, et al. Primary blast injury-induced lesions in the retina of adult rats. *J Neuroinflamm*. 2013;10:79.
10. Yeoh S, Bell ED, Monson KL. Distribution of blood–brain barrier disruption in primary blast injury. *Ann Biomed Eng*. 2013;41:2206–2214.
11. Choi JH, Greene WA, Johnson AJ, et al. Pathophysiology of blast-induced ocular trauma in rats after repeated exposure to low-level blast overpressure. *Clin Exp Ophthalmol*. 2014;43:239–246.
12. Friedlander FG. The diffraction of sound pulses. I. Diffraction by a semi-infinite plane. *Proc Roy Soc London A*. 1946;186:322–344.
13. Cockerham GC, Rice TA, Hewes EH, et al. Closed-Eye ocular injuries in the Iraq and Afghanistan wars. *N Engl J Med*. 2011;364:2172–2173.

14. Mohan K. Retinal ganglion cell damage in an experimental rodent model of blast-mediated traumatic brain injury. *Invest Ophthalmol Vis Sci*. 2013;54:3440–3450.
15. National Ground Intelligence Center. U.S. Army improvised explosive device (IED) safe Standoff Distance cheat sheet. Available at: https://publicintelligence.net/u-s-army-improvised-explosive-device-ied-safe-standoff-distance-cheat-sheet/.
16. Alonso FD, Ferradás EG, Pérez JF, Aznar AM, Gimeno JR, Alonso JM. Characteristic overpressure–impulse–distance curves for the detonation of explosives, pyrotechnics or unstable substances. *J Loss Prevent Process Industries*. 2006; 19:724–728.
17. Pelli DG. The Videotoolbox software for visual psychophysics: transforming numbers into movies. *Spatial Vis*. 1997;10: 437–442.
18. Umino Y, Solessio E, Barlow RB. Speed, spatial, and temporal tuning of rod and cone vision in mouse. *J Neurosci*. 2008;28: 189–198.
19. Cahill H, Nathans J. The optokinetic reflex as a tool for quantitative analyses of nervous system function in mice: application to genetic and drug-induced variation. *PLoS One*. 2008;3:e2055.
20. Brainiard DH. The psychophysics toolbox. *Spatial Vis*. 1997; 10:433–436.
21. Dixon WJ, Mood AM. A method for obtaining and analyzing sensitivity data. *J Am Stat Ass*. 1948;43:109–126.
22. Levitt H. Transformed up-down methods in psychoacoustics. *J Acoustic Soc Am*, 1971;49(Suppl 2):467+.
23. Orlowski J, Harmening W, Wagner H. Night vision in barn owls: visual acuity and contrast sensitivity under dark adaptation. *J Vis*. 2012;12(13):4.
24. Blanco-Mezquita T, Martinez-Garcia C, Proença R, et al. Nerve growth factor promotes corneal epithelial migration by enhancing expression of matrix metalloprotease-9. *Invest Ophthalmol Vis Sci*. 2013;54:3880–3890.
25. Ryan DO, Bennet MM, Sia R, et al. The cornea after primary blast trauma. *Int J Ophthalmol Clin Res*. 2015;2.
26. Dutca LM, Stasheff SF, Hedberg-Buenz A, et al. Early detection of subclinical visual damage after blast-mediated TBI enables prevention of chronic visual deficit by treatment with P7C3-S243. *Invest Ophthalmol Vis Sci*. 2014;55:8330–8341.
27. DeMar J, Sharrow K, Hill M, Berman J, Oliver T, Long J. Effects of primary blast overpressure on retina and optic tract in rats. *Front Neurol*. 2016;7:59.
28. Balaratnasingam C, Morgan WH, Bass L, Cringle SJ, Yu D-Y. Time-dependent effects of elevated intraocular pressure on optic nerve head axonal transport and cytoskeleton proteins. *Invest Ophthalmol Vis Sci*. 2008;49:986–999.
29. Mathews MK, Guo Y, Langenberg P, Bernstein SL. Ciliary neurotrophic factor (CNTF)-mediated ganglion cell survival in a rodent model of non-arteritic anterior ischaemic optic neuropathy (NAION). *Br J Ophthalmol*. 2015;99:133–137.
30. Lin M, Carlson E, Diaconu E, Pearlman E. CXCL1/KC and CXCL5/LIX are selectively produced by corneal fibroblasts and mediate neutrophil infiltration to the corneal stroma in LPS keratitis. *J Leukocyte Biol*. 2007;81:786–792.
31. Cockerham GC, Lemke S, Rice TA, et al. Closed-globe injuries of the ocular surface associated with combat blast exposure. *Ophthalmology*. 2014;121:2165–2172.
32. Heffner RS, Heffner, HE. Visual Factors in Sound Localization in Mammals. *J Comp Neurol*. 1992;317:219–232.
33. Massof RW, Chang FW. A revision of the rat schematic eye. *Vision Res*. 1972;12:793–796.
34. Lozano DC, Twa MD. Development of a rat schematic eye from in vivo biometry and the correction of lateral magnification in SD-OCT imaging. *Invest Ophthalmol Vis Si*. 2013;54:6446–6455.

Investigative Ophthalmology & Visual Science